

# Copper matrix nanocomposites based on carbon nanotubes or graphene

Dawid Janas<sup>a,\*</sup>, Barbara Liszka<sup>b</sup>

<sup>a</sup> *Department of Chemistry, Silesian University of Technology, B. Krzywoustego 4, 44-100 Gliwice, Poland*

<sup>b</sup> *Faculty of Earth Sciences, University of Silesia, 75 Pułku Piechoty 1, 41-500 Chorzów, Poland*

## **Abstract:**

Recently, copper-nanocarbon composites have become the focal point of many research groups around the world. The reason for this phenomenon is that carbon nanotubes or graphene have proven that they can bring the technology of copper to a whole new level due to their extraordinary electrical, thermal and mechanical properties. Addition of even small amounts of nanocarbon into copper matrix can significantly enhance its performance, but unfortunately integration of these two materials is not trivial. In this review article we highlight methods of manufacture of Cu-nanocarbon composites and properties of the resulting material. We stress their strong and weak points as well as indicate pending challenges remaining to be sorted out to produce the nanocomposite of significantly improved properties as compared to neat Cu. Finally, we identify future R&D directions, which must be taken to bring these materials closer to mass-production and eventually real-life applications.

---

\* Corresponding author. Tel: +48 32 2372958. E-mail address: dawid.janas@polsl.pl (D. Janas)

## 1. Introduction

During the last few decades, there has been a growing interest in nanotechnology, which encompasses objects so tiny (of the order of  $10^{-9}$  m) that they are actually quite difficult to imagine. The conception of possibility of materials construction, modification and application on such a small scale, given by the famous lecture “There is plenty of room at the bottom” by American physicist Richard Feynman <sup>1</sup> became an inspiration to taking up the subject for many researches, which continues to this day. Some of the accomplishments were particularly successful in boosting the R&D in this field: the discovery of new forms of carbon such as fullerenes in 1985 <sup>2</sup>, carbon nanotubes (CNTs) in 1991 <sup>3</sup> and graphene in 2004 <sup>4</sup> were particularly successful. Nanotechnology has made since then much wider impact and opened up new horizons in almost all modern disciplines such as materials science <sup>5, 6</sup>, biochemistry <sup>7, 8</sup>, catalysis <sup>9-11</sup>, medicine <sup>12, 13</sup>, various parts of engineering <sup>14-16</sup> and many other.

Bulk copper has been one of the leading choices for applications requiring high performance in terms of electrical and thermal conductivity for hundreds of years. It is the second least resistive metal after silver (copper:  $1.68 \times 10^{-8} \Omega \cdot \text{m}$ , silver:  $1.59 \times 10^{-8} \Omega \cdot \text{m}$ ) <sup>17</sup> with impressive current carrying capacity of the order of  $10^6$  A/cm<sup>2</sup> <sup>18</sup> and the highest thermal conductivity among metals  $398 \text{ W/m}\cdot\text{K}$  <sup>19</sup>. From a practical point of view, it can easily be formed into conductive wires or tracks, which explains its abundance in many applications ranging from microelectronics, overhead power transmission lines, active heat exchangers to heat sinks. Ever since carbon nanomaterials such as CNTs or graphene came into existence, researchers wondered how to utilize their unbeaten electrical and thermal properties to further improve the established technology of copper. Enhancements are necessary to meet the requirements of our modern world wherein the energy demand is growing and its management has to be of the highest

possible efficiency. The research on copper nanocomposites is now in the exponential phase (Fig. 1) and scientific groups from all around the world work on the development of copper-nanocarbon composites of significantly improved properties. In fact, first attempts to integrate copper with carbon (*e.g.* graphite, carbon fiber) took place as early as in 1970s<sup>20, 21</sup> or before.

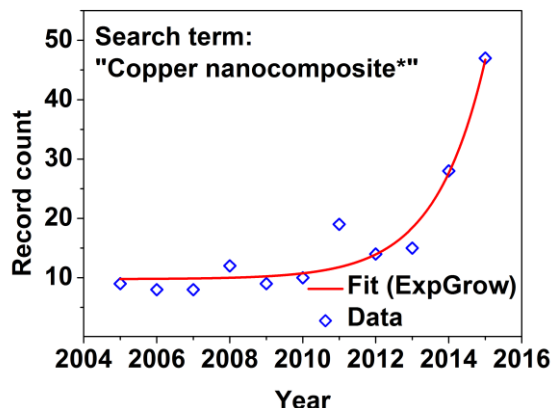


**Fig. 1.** Trends in research on copper nanocomposites represented as number of journal publications in the last 10 years as reported by the Web of Science database.

There is a range of techniques employed to manufacture Cu-nanocarbon composites, but the three most common routes are based on powder metallurgy<sup>22-34</sup>, electroplating<sup>35-45</sup> or electroless deposition<sup>46, 47</sup>. The synthetic approach has to be precisely designed to overcome the problem of the “*cuprophobic*” nature of nanocarbon materials. Due to large surface free energy mismatch (72.9 mJ/m<sup>2</sup> for nanocarbon<sup>48</sup> as opposed to 1650 mJ/m<sup>2</sup> for Cu<sup>49</sup>), these two materials have only slight affinity to each other and often it is hard to combine them without special pretreatment steps to nanocarbon<sup>50</sup> or engaging carbide forming materials at the interface<sup>51</sup>. Although carbide forming metals such as Ti, Co, Cr, V, W or Mo have lower electrical conductivity than Cu they create much better Ohmic interface with unfunctionalized nanocarbon materials<sup>52, 53</sup>. When good contact is obtained between nanocarbon and Cu, the composite

reveals significantly improved properties. For instance, Cu-CNT composites proved to have one hundred-fold higher ampacity (maximum amount of electric current that a conductor can carry without deterioration; often referred to as current-carrying capacity) than pure copper<sup>40</sup> (besides improvements in terms of mechanical and thermal properties). The effect is a result of suppressed electromigration of Cu atoms at high current density and skin effect at high frequency<sup>54</sup>. Encouraging results from other metal matrix composites loaded with CNTs or graphene strongly suggest that the nanocarbon additive may bring enhancement of properties on many fronts<sup>55-58</sup>.

In this review article, we summarize the up to date progress that has been made in the synthesis and evaluation of performance of copper nanocomposites with the focus on CNTs or graphene as the additive to the copper matrix. First, we present what are the successful strategies to combine nanocarbon and copper. Then, we show the electrical, thermal and mechanical properties of the composites. To prove the advantage of using the nanocomposites over traditional materials in these areas, we compare the measured values with neat copper reference recorded using the same setup in each case. Since some properties (*e.g.* Vickers Hardness) are very much dependent on testing parameters, we compared the performance of Cu-nanocarbon composites versus that of neat copper measured under the same conditions (where appropriate data was reported). Finally, we highlight the possible applications and suggest future directions of research.

## 2. Preparation methods

The methods used to combine nanocarbon and copper are mostly based on established techniques such as powder metallurgy, electroplating or electroless deposition. In this section we stress what are their merits, scalability potential and the nature of the material they produce.

### 2.1. Cu-CNT composites

#### 2.1.1. Powder processing

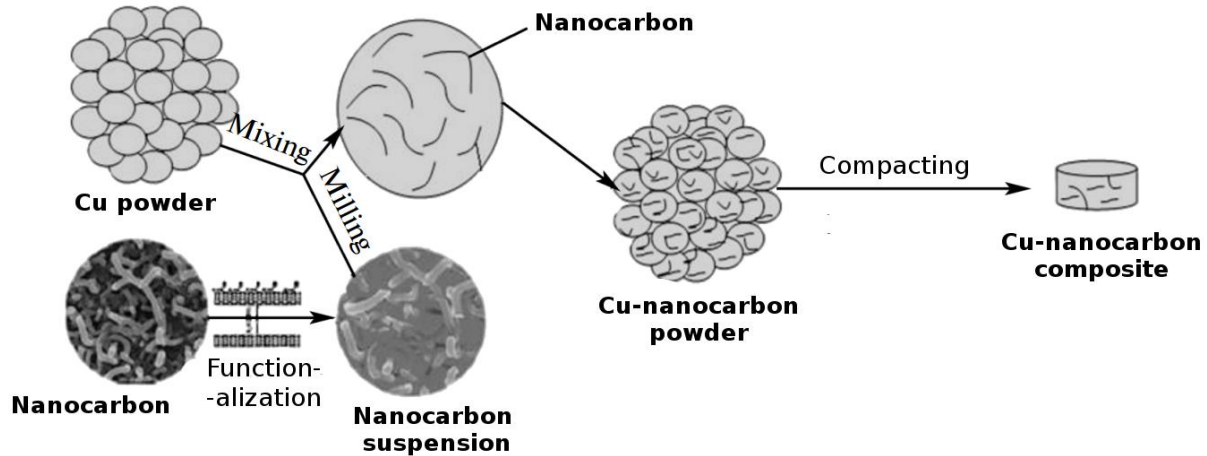


**Fig. 2.** Powder processing route towards Cu-nanocarbon composite. Modified and reproduced with permission. Copyright 2015, Pleiades Publishing Ltd <sup>59</sup>.

Powder metallurgy is the most common approach to create Cu-CNT composites (wherein Cu is the matrix) because of its scalable nature (Fig. 2). Combination of copper and nanocarbon powder is relatively easy to execute and can be accomplished using established and widely available machinery. Arnaud *et al.* used double-wall CNTs (0.5 vol.%), which were pretreated with acid to introduce necessary functional groups for appropriate bonding with copper <sup>22</sup>. Both CNTs and Cu were suspended and sonicated in a liquid medium to ensure homogeneous mixing.

The material was dried, compacted, sintered and used for wire-drawing, which reached lengths up to 1.5 m. The microstructure resembled that of pure Cu, but the Ultimate Tensile Strength (UTS) of the composite was increased by about 10% reaching 560 MPa at room temperature. UTS is a maximum amount of stress a material can withstand during elongation before failure. Moreover, the strain was as high as 7.5% as compared with 6.2% for pure Cu. At the same time, electrical resistivity at room temperature was similar to pure Cu with a slight increase at 77K (about 12%).

Many materials have been considered to enhance the properties of copper, but addition of another phase was often found to increase the scattering rate of the conducting electrons or deteriorate stress transfer capabilities. As a consequence, there is a consensus that the amount of nanocarbon should not be excessive. Another important aspect is homogeneity of CNT distribution and good interfacial bonding to Cu matrix. It was shown that the addition of 5% vol. of double-wall CNTs can increase the Vickers microhardness by more than 50% (up to 82 – as compared with 50 for pure Cu) with a notable decrease in the average friction coefficient <sup>23</sup>. It was observed that increase in the number of CNT walls lowers microhardness. The authors explained this effect by the decrease in packing density with the increase in the number of constituting walls.

In another approach reported by Rajkumar *et al.*, CNTs were first precoated with Cu by electroless deposition and then mixed/compact/sintered according to the regular powder metallurgy route <sup>24</sup> to improve the intermatrix bonding. The results showed that addition of CNTs lowers the wear rate as compare with unreinforced copper. The reason was the formation of carbonaceous film at the contact surface, which introduced lubricating properties into the

material. The nanocomposites also indicated high Vickers microhardness (up to 126), which was 26% harder than regular copper.

Contact between CNTs and copper matrix can be also improved by shearing the composite powder by high-speed rotary blade <sup>25</sup>. It causes interparticle impacting, shearing and friction, which results in coating of the Cu particles with nanocarbon. During the course of composting, CNT assemblies are disintegrated into individual CNTs and used dendritic Cu particles turned into spheres. Despite that good contact between Cu matrix and CNTs, the length of CNT is reduced, which results in imperfect phonon coupling. As a consequence, thermal conductivity of the nanocomposites is slightly inferior to that of pure copper (328 vs 331 W/m·K).

Nevertheless, there are reports utilizing the powder metallurgy route, which show the thermal conductivity of the Cu-CNT composite to be higher than that of copper (359 vs 345 W/m·K). However, thermal conductivity of Cu is commonly given as 400 W/m·K <sup>37</sup>, so further research is needed to confirm whether the measured conductivity of the composite is in fact higher or Cu of inferior quality was used as the reference.

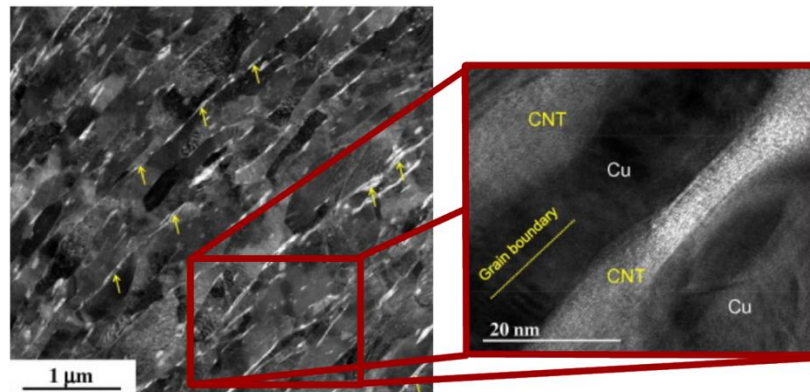


**Fig. 3.** CNTs on the grain boundaries of Cu matrix as observed by bright-field high-resolution TEM. Modified and reproduced with permission. Copyright 2013, Elsevier <sup>27</sup>.

Furthermore, because of the notable anisotropy of CNT electrical/thermal conductivity, which is much higher along the axis than in the radial direction, it is important to align the individual CNTs in the matrix. Yoo *et al.* employed high-ratio differential speed rolling (HRDSR) of Cu-CNT composite sheaths to target this goal (Fig. 3,4) <sup>27</sup>. The Vickers microhardness of the nanocomposite was almost twice that of pure Cu (135 vs 70) whereas the UTS reached 500 MPa (as compared with 400 MPa for Cu measured under the same conditions). The results also showed that ball-milling/rolling degrades the structure of the CNTs therefore it should be used for the shortest possible amount of time to preserve their highly conductive character. Because of high-shear strain induced by HRDSR, the CNTs themselves were found on the grain boundaries within the bulk of Cu matrix (Fig. 3). It is interesting to note that equal speed rolling results in poorly dispersed and scattered CNTs throughout the Cu matrix.

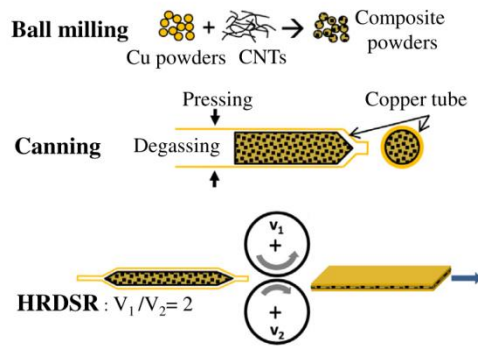


**Fig. 4.** Fabrication procedure of Cu-nanocarbon composite by high-ratio differential speed rolling (HRDSR). Modified and reproduced with permission. Copyright 2013, Elsevier <sup>27</sup>

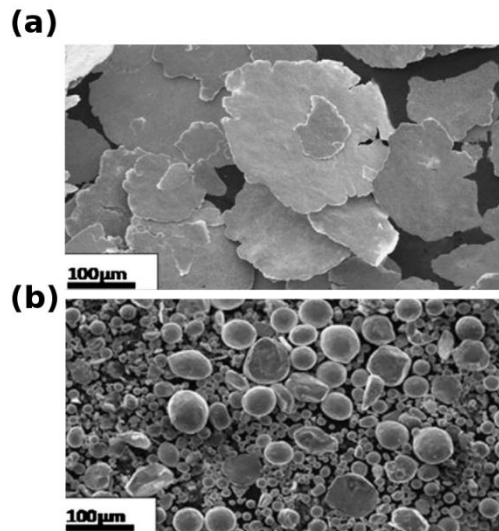


**Fig. 5.** Microstructure of Cu-CNT composites. (a) flake-like. (b) spherical. Modified and reproduced with permission. Copyright 2013, Elsevier <sup>60</sup>.

In all of the cases high-ratio differential speed rolling gave better mechanical properties than the samples prepared by equal speed rolling. Shukla *et al.* showed that hardness of the composites increases with the content of single-wall CNTs, but the opposite was true for multi-wall CNTs. Single-wall CNTs were generally found to have better reinforcement properties <sup>61</sup>. At the same time increase in the CNT content may increase the dislocation density in the composites <sup>59</sup>. Size and shape of copper particles is also important. Dendritic Cu particles give composites with nanocarbon, which have higher microhardness than composites made from spherical Cu particles <sup>62</sup>. What is more, prolonged milling of Cu-CNT mixtures often leads to flake-like morphology of Cu <sup>27, 60, 61</sup> if the content of CNTs is relatively low or excessive milling is carried out (Fig. 5a). With an increased CNT content the Cu particles become smaller and more spherical in shape (Fig. 5b), which has a negative effect on bonding between individual constituents. The bottom line is that the processing power and time has to be optimized. Cu-CNT composites with good

intermatrix bonding should be obtained with minimum disruption to the hexagonal lattice of the CNTs. That ensures improved properties of the nanocomposite as compared with pure Cu.

### 2.1.2. Electrodeposition

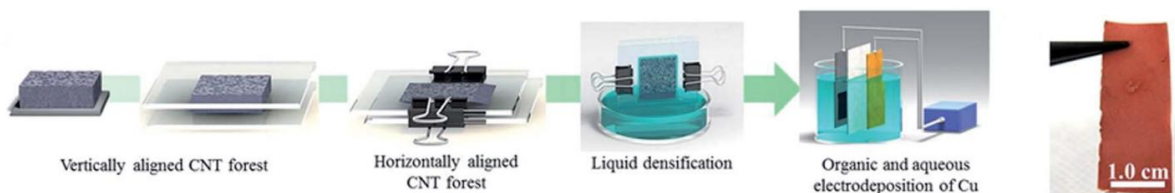


**Fig. 6.** Cu-nanocarbon manufacture by electrodeposition. Modified and reproduced with permission. Copyright 2014, Royal Society of Chemistry <sup>37</sup>.

Another approach to create Cu-CNT nanocomposites is to electroplate one of the ingredients with the other one. Most commonly, CNTs are the target and Cu is deposited using established techniques, wherein aqueous copper sulfate solution is the most common source of Cu atoms, but deposition from organic media is also commonly employed because carbon nanostructures are much easier wetted by them (Fig. 6). Addition of CNTs to Cu was found to lower the Temperature Coefficient of Resistance (TCR) <sup>35</sup> because of the inherently low sensitivity of their electrical resistance to temperature <sup>14</sup> (tested from 50 to 350K). Similarly as in the case of powder metallurgy route, Cu-CNT composites prepared by electrodeposition have improved properties as compared to pure Cu. The tensile strength, yield strength and ampacity are increased by 49%, 95% and 32%, respectively (super-aligned CNT arrays were electroplated in an aqueous Cu bath) <sup>35</sup>. Thermal conductivity surpassed that of copper and reached up to 427 W/m·K. Furthermore, a continuous process of CNT deposition with Cu was shown by Xu *et al* <sup>36</sup>. CNT fibers produced by direct spinning <sup>63</sup> are spun and passed through anodization and deposition baths to fabricate a composite wire. Nanocomposite of high UTS was obtained (811

MPa, as compared with Cu wires), which is partially caused by the starting material (CNT fiber substrate) of very good mechanical properties. CNT fibers produced by this method are known for its high-strength<sup>64</sup>, which should be taken into the account. Unfortunately the reported values of electrical conductivity of these nanocomposites (up to  $2.45 \times 10^{-5} \Omega \cdot m$ ) are inferior to similar materials produced by different methods.

Another interesting property of Cu-nanocarbon composite is its exceptionally low Coefficient of Thermal Expansion (CTE). When CNTs, which have negative CTE<sup>65</sup>, are electroplated with Cu of positive CTE<sup>66</sup>, the resulting material has 70% lower CTE than most metals<sup>37</sup>. The net effect gives silicon-like CTE on the order of 5 ppm/K. Because of its high thermal conductivity (395 W/m·K) and negligible CTE mismatch with silicon, the nanocomposite has been considered as a promising heat sink for CPUs and other silicon-based circuits, which generate heat inside of computers.

What regards the process of electrodeposition, a variety of modifications have been devised to improve it. For instance, Feng *et al.* described co-depositon of Cu and CNTs onto a substrate with nanodiamonds used as a dispersing agent to prevent agglomeration of CNTs<sup>38</sup>. The authors claim that nanodiamonds help to mitigate agglomeration of CNTs in polymer matrices<sup>67</sup>, but the merits of using them for electrodeposition were not shown. Next, electrodeposition by periodic pulse reverse had a positive effect on the speed of the deposition, but the conductivity of the nanocomposite was inferior to that of prepared by DC electroplating. Moreover, Cu-CNT composites prepared by electrodeposition also have improved microhardness as compared to pure copper. An increase by up to 36% was observed<sup>39</sup>. Probably the most notable improvement in properties, which justifies combination of Cu and CNTs on an industrial scale, comes from the results of Subramaniam *et al.*<sup>40, 41</sup>. In a two step process, CNTs were first electroplated with Cu

seeds using organic medium (copper acetate in acetonitrile) and then electrodeposition from typical aqueous solution was employed. Organic media are much better for infiltration of hydrophobic CNTs to precoat them with Cu seeds, from which Cu clusters can grow in the subsequent step. The team has shown that Cu-CNT nanocomposite can have two orders of magnitude higher ampacity, an order of magnitude lower TCR and similar electrical conductivity as compared with pure Cu. Electromigration of Cu, the primary cause of failure at high current, was suppressed to a large extent. At this level, the Cu-CNT composite already shows significant competitive advantage. It is probably most evident in terms of specific conductivity, which takes into account weight of a conductor. Because of high electrical conductivity, but low density of CNTs the Cu-CNT composite has got 26% higher specific conductivity than pure Cu.

Next, as stressed by Hannula *et al.*, to prepare Cu-CNT nanocomposites of appreciable properties by electrodeposition, two issues must be overcome. Firstly, the current distribution throughout CNT macroassembly is often non-uniform<sup>68</sup>, which causes excessive nucleation close to the electrodes, but insufficient beyond a certain distance from a current feed point due to a large voltage drop. Ideally, CNT macroassemblies such as fibers or films, which are the target for the Cu electrodeposition, should be of low resistivity to alleviate this problem. Secondly, similarly as in the case of powder metallurgy route, the CNTs should have some degree of functionalization<sup>50</sup> to improve the interaction with Cu. Such functionalization again should not be too severe not to disrupt the  $sp^2$ -network of carbon atoms, which allows for efficient transport of charge carriers.

### 2.1.3. Electroless deposition

The route involving electroless deposition is relatively unexplored. In an electroless plating, metals are deposited onto a given surface without use of external electrical power, but instead the process is driven by a chemical reaction (Fig. 7). A typical mixture of copper sulfate (Cu source), glyoxylic acid (reducing agent) and EDTA (ethylenediaminetetraacetic acid, complexing agent) was employed to manufacture homogeneous Cu-CNT composites, but unfortunately the properties of these composites were not examined<sup>69, 70</sup>. The authors stressed the importance of appropriate dispersion of CNTs, which enables uniform coating with Cu. Out of magnetic stirring, ultrasonic homogenization and atomization, the last approach yielded the best results. Nevertheless, CNTs were uniformly covered with Cu in the plating bath. CNTs of different size are equally well covered with Cu as long as they are properly dispersed (with the assistance of an appropriate surfactant *e.g.* sodium dodecyl sulfate).

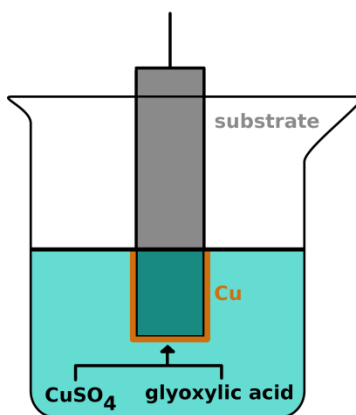


**Fig. 7.** Electroless deposition of Cu onto a flat substrate.

A summary of the properties of the Cu-CNT composites is given in Table 1.

Preparation method	CNT		Best properties			Ref.
	Content	Type	Electrical	Thermal	Mechanical	
Powder processing	0.5 vol.%	DWCNTs	$\rho: 2.03 \times 10^{-8} \Omega \cdot m$ ( $1.95 \times 10^{-8}$ )	N/A	<b>UTS: 560 MPa (450)</b> <b><math>\delta: 7.5\%</math> (6.2)</b>	22
	0–10 vol.%	DWCNTs MWCNTs	N/A	N/A	HV: 82 (50)	23
	0–20 vol.%	MWCNTs	N/A	N/A	HV: 126 (100)	24
	0–10 vol.%	MWCNTs	N/A	$\kappa: 328 \text{ W/m}\cdot\text{K}$ (331)	N/A	25
	0–10 vol.%	MWCNTs	N/A	$\kappa: 359 \text{ W/m}\cdot\text{K}$ (345)	N/A	26
	0–3 vol.%	MWCNTs	N/A	N/A	UTS: 500 MPa (400) HV: 135 (70)	27
Electro-deposition	0–1 vol.%	MWCNTs	$\rho: 2.33 \times 10^{-8} \Omega \cdot m$ $a: 1.17 \times 10^4 \text{ A/cm}^2$	<b><math>\kappa: 427 \text{ W/m}\cdot\text{K}</math> (400)</b>	UTS: 282.7 MPa (168) $\delta: 4\%$ (13)	35
	N/A	MWCNTs	$\rho: 2.45 \times 10^{-5} \Omega \cdot m$	N/A	<b>UTS: 811 MPa</b>	36
	45 vol.%	MWCNTs	N/A	$\kappa: 395 \text{ W/m}\cdot\text{K}$ (400)	CTE: 5 ppm/K (16)	37
	N/A	MWCNTs	$\rho: 3 \times 10^{-8} \Omega \cdot m$ ( $1.7 \times 10^{-8}$ )	N/A	N/A	38
	0–10 vol.%	SWCNTs	<b><math>\rho: 1.65 \times 10^{-8} \Omega \cdot m</math></b> <b>(<math>1.67 \times 10^{-8}</math>)</b> <b><math>\alpha: 6.20 \times 10^{-3} \text{ 1/K}</math></b> <b>(<math>6.80 \times 10^{-3}</math>)</b>	N/A	<b>HV: 164 (120)</b>	39
	45 vol.%	SWCNTs	$\rho: 2.12 \times 10^{-8} \Omega \cdot m$ ( $1.72 \times 10^{-8}$ ) <b><math>a: 6 \times 10^8 \text{ A/cm}^2</math></b> <b>(<math>6 \times 10^6</math>)</b>	N/A	N/A	40, 41

**Table 1. The summary of properties of Cu-CNT composites. Corresponding values for pure Cu are given in parentheses. Shaded cells indicate nanocomposites with the highest enhancement of properties as compared with pure Cu.**

$\rho$  (electrical resistivity),  $a$  (ampacity),  $\alpha$  (temperature coefficient of resistance),  $\kappa$  (thermal conductivity), UTS (Ultimate Tensile Strength), HV (Vickers Hardness),  $\delta$  (elongation to fracture),  $E$  (Young's modulus),  $\sigma$  (flexural strength), CTE (Coefficient of Thermal Expansion).

The highest recorded performance in each categories are:  $\rho$ :  $1.65 \times 10^{-8} \Omega \cdot m$ , ampacity:  $6 \times 10^8$  A/cm<sup>2</sup>,  $\kappa$ : 427 W/m·K,  $\alpha$ :  $6.20 \times 10^{-3}$  1/K, UTS: 811 MPa,  $\delta$ : 7.5% and HV: 164. As compared with Cu matrix, the biggest improvements are in the area of electrical properties. Ampacity was increased by two orders of magnitude. Moreover, the material had enhanced mechanical properties (especially Vickers Hardness), which almost doubled. There was also evident increase in UTS. Unfortunately, possibly due to imperfect phonon coupling, the increase in thermal conductivity of Cu-CNT composites was only marginal. A summary of the improvements is presented in the Fig. 8. The data show that electrodeposition gives stronger enhancement of properties of the nanocomposite as compared with pure Cu (Table 1.) Nanocomposites prepared by powder processing are mostly improved in terms of their mechanical properties.

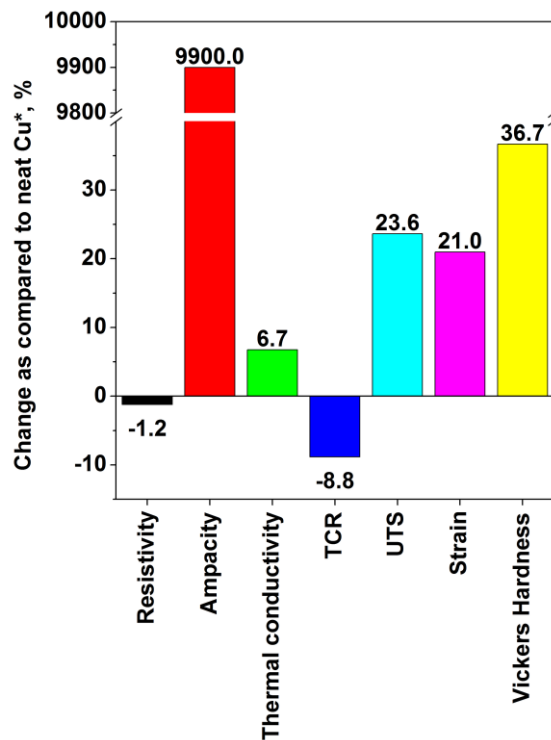


**Fig. 8.** Performance of Cu-CNT composites as compared to pure Cu. \*UTS of the CNT-Cu composite is compared to CNT fiber, on which Cu is deposited.

## 2.2. Cu-graphene composites

### 2.2.1. Powder processing

Similarly as in the case of CNTs, powder metallurgy route is the most common method for the preparation of Cu-graphene composites. Graphene flakes also need functional groups to facilitate appropriate bonding with the Cu matrix. Gao *et al.* reported a technique wherein graphene oxide is additionally positively charged with hexadecyltrimethylammonium bromide (CTAB) which helps in its uniform distribution in the composite <sup>28</sup>. Addition of graphene improves thermal conductivity (up to 396 W/m·K as compared with 360 W/m·K for Cu), UTS (up to 210 MPa as compared with 185 MPa for Cu) and the Vickers Hardness (up to 51 as compared with 43 for Cu). The enhancement gradually increases with the content of graphene up to 0.3 wt% and then starts to decline with further addition of carbon nanomaterial. Excessive amount of nanocarbon does not act as reinforcement anymore, but introduces defects and dislocations which deteriorate the phonon propagation and stress transfer. Furthermore, it was shown that the addition of graphene gives radically different results than incorporation of its parent material graphite. Graphene based composite exhibits much higher microhardness and bending strength. Moreover, the wear rate is significantly reduced <sup>29</sup>. The results show once again that nanoscopic structure of the additive is crucial for the improvement of properties of the matrix. Such structure also has to be carefully optimized. Dutkiewicz *et al.* reported that fine graphene flakes give about 50% higher hardness and 30% lower resistivity of the composite than the composite prepared with coarse graphene particles <sup>30</sup>. The explanation was that the finer flakes are more homogeneously distributed within the Cu matrix whereas the coarse ones prefer to reside at the grain boundaries. It was shown that to preserve beneficial electrical, thermal and mechanical properties of the filler, pristine graphene may be used instead of graphene oxide under certain circumstances <sup>31</sup>.

Sequential addition and removal of polyvinylpyrrolidone (to disperse graphene in copper matrix) leads to composite having 84% IACS (the International Annealed Copper Standard) in terms of electrical conductivity, but much higher compression and yield strength than pure Cu. Addition of graphene in general has significant influence on the mechanical properties and gradually changes the fracture mechanism from ductile to brittle.

It must be noted that even starting with nanocarbon of high crystalline order, one must be careful what kind of processing is involved up to the final step of the composite manufacture. Often, ball-milling, sonication, shear mixing or other fragmentation technique introduces defects and/or breaks down the constituents (individual CNTs or graphene flakes) into much smaller pieces<sup>32</sup>. Even if it will make the material more processable, the properties of the resulting copper matrix composite may be inferior. An alternative to improve the interaction between nanocarbon and copper is to precoat one of the constituents with a thin layer of transition metal such as nickel or chromium, which has affinity towards both of the nanocomposite constituents<sup>71</sup>. Although it is not ideal for the electrical applications because the conductivity of Ni or Cr is much lower than that of Cu or nanocarbon, the results have shown that such addition is suitable where improved mechanical properties are wanted. Ni-graphene-Cu composite had 64.5% higher yield strength than regular Cu<sup>47</sup>. To eliminate the influence of other components than graphene and Cu, the graphene flakes may be precoated with Cu nanoparticles by electroless deposition and then subjected to powder metallurgy processing<sup>46</sup>. UTS as high as 485 MPa was achieved using this approach. In terms of the highest absolute values, yield strength of 501 MPa was reported<sup>72</sup>, which is on par with the previously described best results for Cu-CNT composites.

### 2.2.2. Electrodeposition

To synthesize the Cu-graphene nanocomposite by electroplating the typical copper sulfate approach is employed. Jagannadham showed how Cu seeds and graphene oxide can be co-deposited onto an electrode to form the composite <sup>43</sup>. The material revealed higher thermal conductivity than copper (460 vs 380 W/m·K) at room temperature. The difference was even more evident at 250 K (510 vs 400 W/m·K). The study of electrical properties indicated that the composites have a slightly lower resistivity (up to 11% as compared with electrolytic copper) and reduced TCE (as in the case of CNTs). To reach the highest thermal or electrical conductivity, a different ratio of graphene has to be introduced into the copper matrix <sup>45</sup>, so the material can be tailored for a particular application. Finally, when graphene flakes are arranged in plane of the composite, thermal conductivity is much higher along this axis rather than normal to the surface as expected. To achieve high isotropic thermal conductivity, random orientation of graphene flakes is preferred <sup>73</sup>.

### Other methods

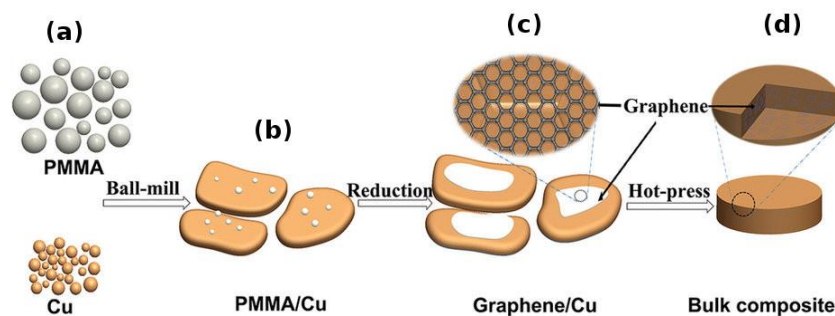


**Fig. 9.** Schematic diagram of the fabrication procedures of graphene/Cu composites. (a) Original Cu powders and poly(methyl methacrylate) (PMMA). (b) Flaky Cu powders loaded with PMMA

after ball-milling. (c) Graphene/Cu composite powders. (d) Bulk graphene/Cu composite after hot-press sintering. Modified and reproduced. Copyright 2016, Nature Publishing Group <sup>34</sup>.

An interesting approach was presented by Chen *et al.*, who mixed Cu powder and PMMA as the graphene precursor, which was then grown in-situ <sup>34</sup> (Fig. 9). The material was then subjected to regular powder metallurgy processing and analyzed. Such technique ensured very good dispersion of the nanocarbon material and good combination between graphene and Cu matrix. Although just a small increase in Hardness was observed, the Yield strength tripled and reached 144 MPa (as compared with 52 MPa for pure Cu). That once again proves that nanocarbon addition strengthens and toughens the Cu matrix.

Another technique to achieve this goal is to use a reported bioinspired strategy <sup>74</sup> (Fig. 10). Nacre-like reduced graphene oxide reinforced Cu matrix composite was prepared by a brick-and-mortar impregnation process. In this case not only the mechanical properties of copper were improved to a large extent, but the inherently high electrical conductivity was preserved.

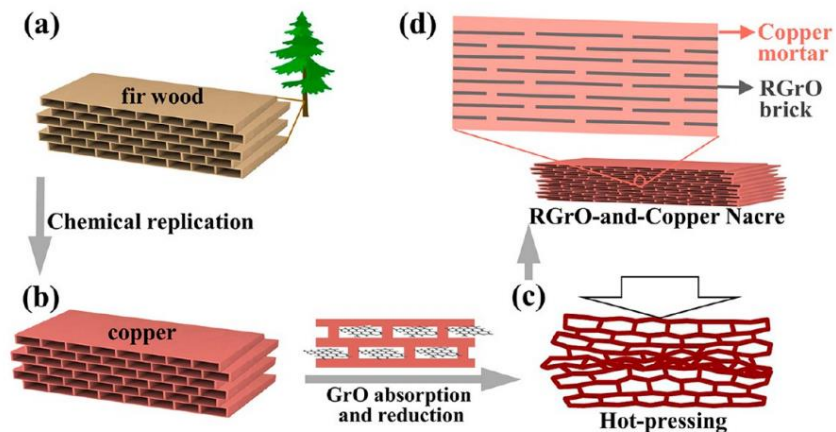


**Fig. 10.** Schematic representation of fabricating RGrO-and-copper artificial nacre. (a) Ordered porous structure in natural fir wood. (b) Replicating the porous structure of fir wood with Cu. (c)

Hot-pressing porous Cu preform absorbed with RGrO. (d) RGrO-and-Copper nacre consisting of RGrO “brick” and copper “mortar”. RGrO stands for reduced graphene oxide. Modified and reproduced with permission. Copyright 2015, American Chemical Society <sup>74</sup>.

A summary of the properties of the Cu-graphene composites is given in Table 2. The highest recorded performance in each category are:  $\rho$ :  $1.7 \times 10^{-8} \Omega \cdot m$ ,  $\alpha$ :  $3.03 \times 10^{-3} K^{-1}$ ,  $\kappa$ : 500 W/m·K, UTS: 485 MPa, Yield strength: 501 MPa,  $\delta$ : 45%, HV: 98. In case of graphene composites, we see that similarly to Cu-CNT composites the electrical conductivity of Cu is reached but no significant improvement is observed. However, in the case of Cu-graphene we see a notable increase in thermal conductivity, which was as high as 500 W/m·K. What regards mechanical properties, enhancement in terms of UTS and Vickers Hardness is only marginal contrary to the results from Cu-CNT composites. The exception is the Yield strength, which almost tripled upon graphene incorporation. A summary of the enhancements is given in the Fig. 11. Similarly as in the case of CNT-based composites, powder processing gives mostly improvements in terms of mechanical properties, whereas electrodeposition enhances electrical and thermal performance.

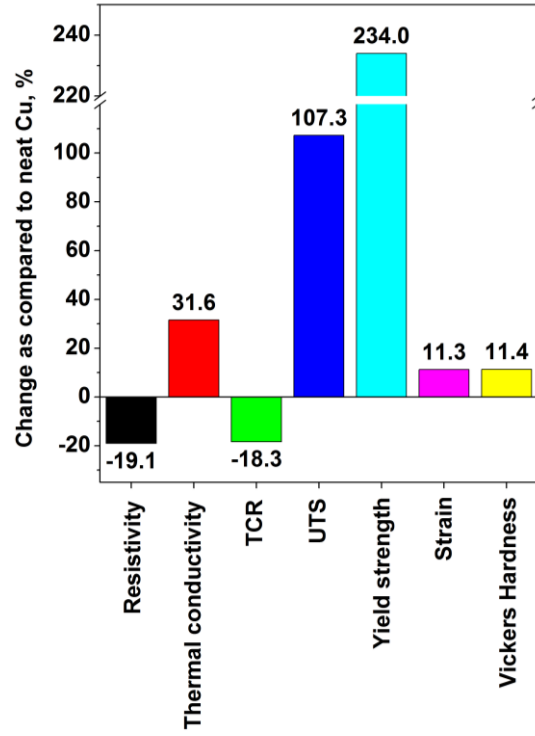


**Fig. 11.** Performance of Cu-graphene composites as compared to pure Cu.

Preparation method	Graphene		Best properties			Ref.
	Content	Type	Electrical	Thermal	Mechanical	
Powder processing	0 – 0.5 wt%	GO	N/A	$\kappa$ : 396 W/m·K (360)	UTS: 210 MPa (185) $\delta$ : 17% (22) HV: 51 (43)	28
	0 – 10 vol.%	G	N/A	N/A	HV: 97 $\sigma$ : 441 MPa	29
	0 – 2 wt%	G, RGO	$\rho$ : $2.3 \times 10^{-8} \Omega \cdot m$	N/A	HV: 62	30
	0 – 0.3 wt%	G, GO	$\rho$ : $2.1 \times 10^{-8} \Omega \cdot m$ ( $1.74 \times 10^{-8}$ )	N/A	UTS: 187 MPa (209)	31
	0 – 2 wt%	GO	N/A	N/A	UTS: 230 MPa (180) $\delta$ : 24% (22) HV: 51 (45)	32
	0 – 6 wt%	RGO	3% increase in electrical conductivity	N/A	<b>HV: 98 (88)</b>	33
	0 – 0.5 vol.%	G	N/A	N/A	UTS: 275 MPa (220) $\delta$ : 20% (32)	47
	1.3 wt%	GO	N/A	N/A	<b>UTS: 485 MPa (234)</b> $\delta$ : 9% (25) E: 104 (85) GPa	46
	0 – 4.8 vol.%	RGO	N/A	N/A	Yield strength: 501 MPa (150)	72

Electro-deposition	N/A	GO	N/A	$\kappa$ : 460 W/m·K (390)	N/A	43
	N/A	GO	$\rho$ : $1.91 \times 10^{-8} \Omega \cdot m$ ( $2.2 \times 10^{-8}$ ) $\alpha$ : $3.03 \times 10^{-3} 1/K$ ( $4.04 \times 10^{-3}$ )	N/A	N/A	44
	N/A	GO	$\rho$ : $1.7 \times 10^{-8} \Omega \cdot m$ ( $2.0 \times 10^{-8}$ ) $\alpha$ : $3.53 \times 10^{-3} 1/K$ ( $3.81 \times 10^{-3}$ )	$\kappa$ : 500 W/m·K (380)	N/A	45
In-situ growth of graphene	0 – 0.95 wt%	G	$\rho$ : $1.7 \times 10^{-8} \Omega \cdot m$ ( $1.8 \times 10^{-8}$ )	N/A	UTS: 274 MPa (215) Yield strength: 144 MPa (52) $\delta$ : 45% (40) HV: 143 (123)	34
Template impregnation	N/A	RGO	$\rho$ : $1.77 \times 10^{-8} \Omega \cdot m$ ( $1.81 \times 10^{-8}$ )	N/A	UTS: 300 MPa (200) $\delta$ : 20% (17)	74

**Table 2. The summary of properties of Cu-graphene composites. Corresponding values for pure Cu are given in parentheses. Shaded cells indicate nanocomposites with the highest enhancement of properties as compared with pure Cu.**

G (graphene), GO (graphene oxide), RGO (reduced graphene oxide),  $\rho$  (electrical resistivity),  $\alpha$  (temperature coefficient of resistance),  $\kappa$  (thermal conductivity), UTS (Ultimate Tensile Strength), HV (Vickers Hardness),  $\delta$  (elongation to fracture), E (Young's modulus),  $\sigma$  (flexural strength).

### 3. Modelling

Results of computation support the experimental findings. In a study by Park *et al.*, the authors prove that oxygen-containing functional groups such as hydroxyl (-OH) or carboxyl (-COOH) or structural defects enhance the interaction between Cu and nanocarbon<sup>75</sup>. The binding energy of Cu on the oxidized CNTs increases in the case of pristine CNT (from -0.53 to -0.73 eV) as well as Stone-Wales defective CNT (from -1.26 to -2.70 eV). In addition to structural integrity, defects and functional groups promote electron exchange between Cu and carbon atoms. According to calculations, 1.9 – 2.4 Å is the optimum distance between nanocarbon and Cu.

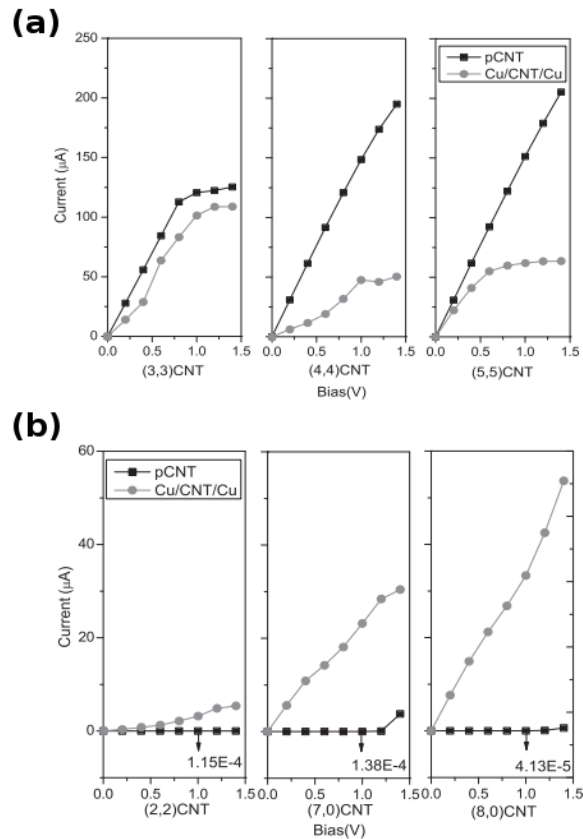


**Fig. 12.** Calculated I-V curves for (a) metallic and (b) semiconducting pristine CNTs (pCNT) and Cu-CNT interconnects (Cu/CNT/Cu) of a given chirality. Modified and reproduced with permission. Copyright 2011, Elsevier<sup>76</sup>.

A strong interaction between O and Cu was detected. In fact,  $O_{2p}$  orbital had extensive overlap with  $Cu_{3d}$  orbital, which confirms favorable interaction. On the other hand, according to Wu *et al.*, pristine nanocarbon interacts with Cu through  $C_{2p}$  orbital and the strength of that interaction is very much dependent on the chirality of a particular CNT. The consequence of that is a radically different shape of calculated I-V curves for various types of Cu-CNT interconnects (Fig. 12).

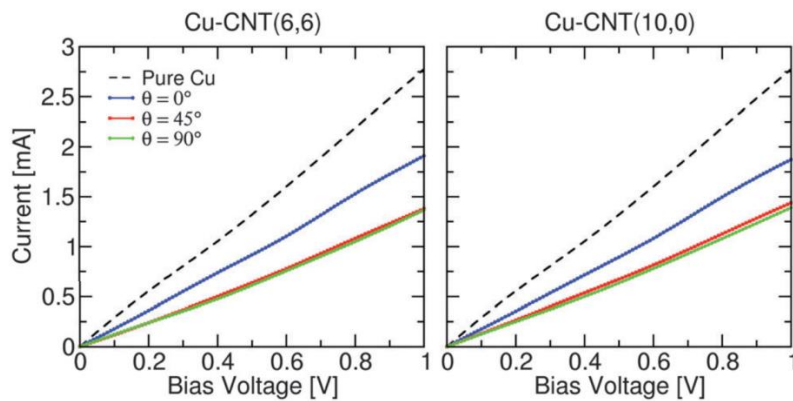


**Fig. 13.** Current–voltage characteristics of Cu–CNT composites with different chirality and orientation. The characteristic of infinite pure Cu is also shown for comparison Modified and reproduced with permission. Published by the PCCP Owner Societies <sup>77</sup>.

The more aligned CNTs in the composite the more homogeneous is the current distribution density at high frequency. On the macroscopic scale, the CNT length <sup>78</sup>, alignment and density in fact play a key role in electrical conductivity of the composite rather than the chirality <sup>77</sup> (Fig. 13). Electrons are injected at the ends of a nanotube rather than the side (as shown in the calculated I-V curves in Fig. 14), therefore misalignments of individual CNTs (or graphene flakes <sup>79</sup>) from the applied bias axis have a deleterious effect on the electrical conductivity.

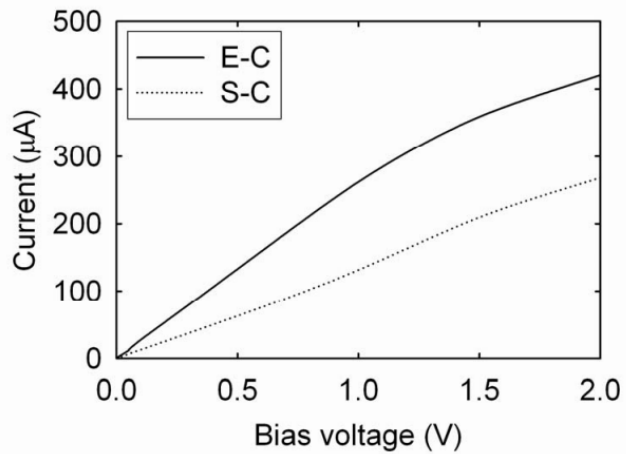


**Fig. 14.** Current–voltage characteristics of Cu–CNT composites with end-contacts (E-C) and side-contacts (S-C). Modified and reproduced with permission. Copyright 2010, American Institute of Physics <sup>80</sup>.

The length of individual CNTs should ideally be above 10  $\mu\text{m}$  <sup>78</sup> and the diameter within the range of >2 nm (for SWCNTs ) and 30-100 nm (for MWCNTs) for the effective resistivity to be optimal (Fig. 15) <sup>54</sup>.

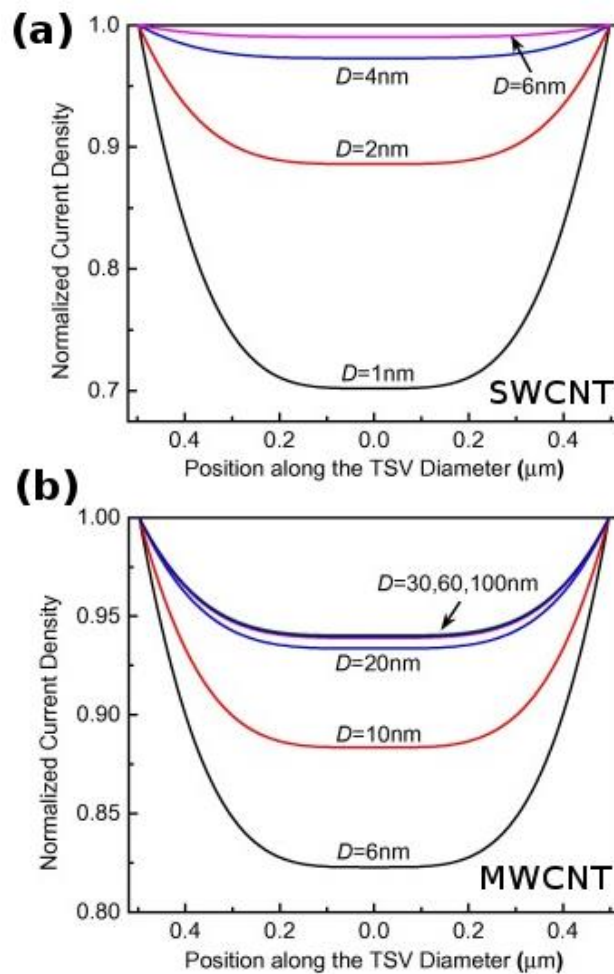


**Fig. 15.** Normalized current density vs position along the conductor diameter for (a) SWCNT and (b) MWCNT of  $D$  diameter. Modified and reproduced with permission. Copyright 2015, Elsevier <sup>54</sup>

Another crucial factor determining the properties of the resulting composite is the structural perfection of the constituting species. A detailed study by Sadowski *et al.* shows that inclusions of adulterants such as graphite or defects can make a significant negative influence on the performance of the Cu-nanocarbon composite in a variety of applications <sup>79</sup>, so the material functionalization level has to be kept at the necessary minimum. Lastly, the presence of

nanocarbon greatly reduces the skin effect<sup>54, 81</sup>, which was later proven experimentally<sup>82, 83</sup>. The skin effect decreases with increasing content of nanocarbon (Fig. 16). Such result can be fundamental for the application of Cu-nanocarbon composites for high-frequency AC transmission.

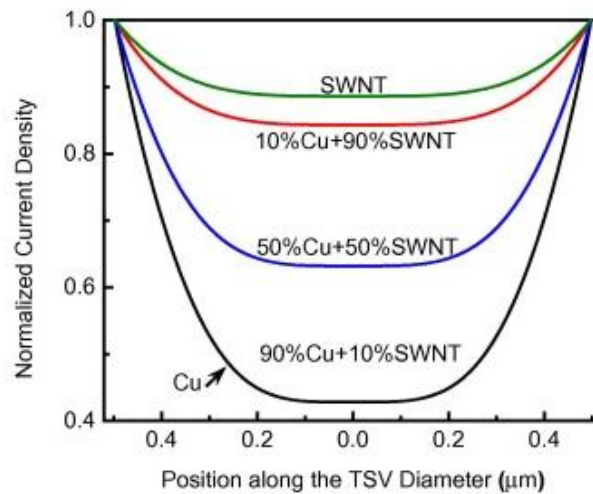


**Fig. 16.** Normalized current density vs position along the conductor diameter as a function of SWCNT content in a Cu matrix. Modified and reproduced with permission. Copyright 2015, Elsevier<sup>54</sup>

What is interesting from the conduction mechanism point of view, the modeling shows that for small diameter CNTs only the metallic ones contribute to current conduction according to the results of Feng *et al.*<sup>54</sup>

#### 4. Applications

Cu-nanocarbon composites have a wide range of possible applications. One of the advantages in adding CNTs or graphene to Cu is the reduced weight of the resulting composite. Highly thermally and electrically conductive nanotubes or graphene flakes of low-weight can substitute

certain amount of Cu to reach the same performance. Probably the most obvious application for such composite is in the transport industry for automotive and aerospace applications. Even small reduction in weight would result in massive savings as these vehicles contain kilograms and tonnes of Cu wiring, respectively. Another area which could gain from using these materials is thermal management. At present, heat sinks are most commonly made from Cu, which is heavy and prone to cracking if subjected to repeated bending. Addition of carbon nanostructures, which are very flexible and produce light-weight nanocomposites with Cu of improved thermal conductivity would be beneficial. Mechanical reinforcement of Cu could be advantageous for other applications as well. Furthermore, carbon nanomaterials are much better suited for the application in extreme environments wherein corrosive chemicals are present<sup>84, 85</sup>. Addition of a protective layer from CNTs or graphene onto Cu or Cu-nanocarbon composite would enable the use of such conductors in the areas where Cu is currently unsuitable.

## **5. Conclusions and future outlook**

In this paper we reviewed the up to date progress in the synthesis and properties of Cu-nanocarbon composites. CNTs or graphene can be combined with Cu matrix by various methods, but most commonly powder metallurgy, electroplating or electroless deposition are employed. These techniques are scalable and proven at industrial level in many parts of engineering. That is very important for the possibility of mass-production of Cu-nanocarbon composites of significantly improved properties in the future. One could also consider exploring how to integrate nanocarbon into the existing other large scale copper technologies such as casting.

The nanocomposites have shown advantages on many fronts, but certain aspects have to be taken care of to make these efforts worthwhile. Firstly, the cost of nanocarbon (in particular graphene and single-wall CNTs) still has to be reduced to a large extent, so that the benefits of the use of

nanocomposite (as compared to pure Cu) are justified from the economic point of view. Over the years we have seen a significant decrease in the unit cost of multi-wall CNTs and increase in their production capacity. At the end of the day, the same has to be the case for single-wall CNTs and graphene to bring these Cu-matrix nanocomposites to a wider audience. Secondly, the production of Cu-nanocarbon composite requires very high-degree of control over the microstructure and composition of the nanocarbon feed. We need to have means of consistent large-scale manufacture of CNTs or graphene of particular length/diameter/number of walls/chirality/*etc.* or flake size/number of layers/*etc.*, respectively, both having the desired surface chemistry. Only such level of control can enable implementation of Cu-nanocarbon composites in the real-life.

The nanocomposites have revealed potential to enhance several Cu parameters, the most notable being: electrical (ampacity), mechanical (hardness, tensile strength) and thermal (thermal conductivity, TCR, CTE) properties. With adequate level of production control we can imagine tailoring the nanocomposite to create a family of Cu-nanocarbon materials for a spectrum of possible applications such as in high-performance wiring or lighter flexible heat sinks for consumer electronics. That is why manufacture method of the nanocomposite should be selected according to which properties of copper should be enhanced. In general, powder processing methods have produced nanocomposites of improved mechanical properties, whereas electrodeposition has enhanced electrical and thermal performance. As we compare copper matrix composites loaded with CNTs and graphene, we see that CNT-based materials have better mechanical properties both in terms of Vickers Hardness (164 *vs* 98) and UTS (811 *vs* 485 MPa), which are almost twice as big as the corresponding values for graphene. On the other hand, graphene-reinforced copper is more thermally conductive (500 *vs* 421 W/m·K) and has got a

lower TCR ( $3.03 \times 10^{-3}$  vs  $6.20 \times 10^{-3}$  1/K). Electrical conductivity of Cu-CNT and Cu-graphene nanocomposites is on par. It is important to note that for the comparison to be accurate, the composites should have been characterized under the same conditions (the quoted values come from different studies). Because the outermost layer contributes the most to current conduction in CNTs, it is not surprising to see that SWCNTs gave the best composites with Cu in terms of electrical conductivity. From the mechanical point of view, very high tensile strength of MWCNTs<sup>86</sup>, translated into excellent reinforcement of Cu matrix. What regards graphene, it would be vital to carry out a study to investigate how the number of layers influences the properties of its composite with Cu. We currently know that fine graphene gives composites with Cu of much higher hardness and lower resistivity<sup>30</sup>, so maybe targeting single layer graphene Cu matrix composites is the route towards the best performance.

What is more, it would be interesting to see the performance of Cu-nanocarbon composites, in which instead of functionalization carbide forming materials such as Ti or Co would be used for improved bonding between the two materials. Such experiments would enable quantification whether the performance of the composite is better when carbon nanomaterials are oxidized or a part of them is converted to connecting carbide layer.

### **Acknowledgments**

D.J. kindly acknowledge National Science Center, Poland (under the Polonez program, grant agreement UMO-2015/19/P/ST5/03799) and the European Union's Horizon 2020 research and innovation programme (Marie Skłodowska-Curie grant agreement 665778). D.J. would also like to thank Foundation for Polish Science for START scholarship (START 025.2017).

### **Conflict of interest**

There are no conflicts of interest to declare.

## Biographies



Dr Dawid Janas graduated from University of Cambridge in 2014 with a PhD degree in materials science. For the next 2 years, he held a Research Associate position in the Electric Carbon Nanomaterials group at the University of Cambridge. Since 2016, he is a Research Fellow at the Silesian University of Technology in Poland. His current research interests include manufacture of carbon nanostructures, tuning of their properties, chemical functionalization and real-life applications.



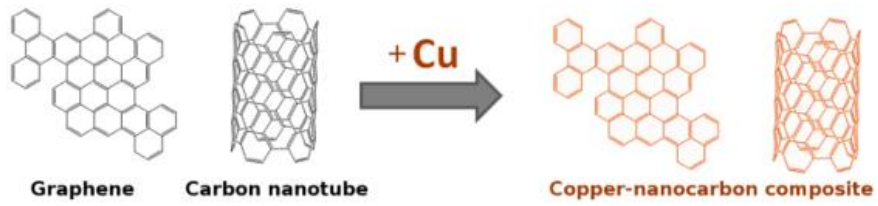
Barbara Liszka is a Research Associate at the University of Silesia in Poland. During 2015 and 2016, she carried out experimental work at the University of Cambridge on the development of functional carbon nanostructure coatings for aerospace industry. Her research interests are focused on the decoration of carbon nanotubes and graphene with metal nanoparticles. She is also involved in development of various applications of glassy carbon.

# Table of contents

## Copper matrix nanocomposites based on carbon nanotubes or graphene

Dawid Janas\* and Barbara Liszka

This review provides an in-depth overview of the production of Cu-nanocarbon composites



## References

1. R. P. Feynman, *Engineering and Science*, 1960, **23**, 22-36.
2. H. W. Kroto, J. R. Heath, S. C. O'Brien, R. F. Curl and R. E. Smalley, *Nature*, 1985, **318**, 162-163.
3. S. Iijima, *Nature*, 1991, **354**, 56-58.
4. K. S. Novoselov, A. K. Geim, S. V. Morozov, D. Jiang, Y. Zhang, S. V. Dubonos, I. V. Grigorieva and A. A. Firsov, *Science*, 2004, **306**, 666-669.
5. Y. L. Li, I. A. Kinloch and A. H. Windle, *Science*, 2004, **304**, 276-278.
6. X. F. Zhang, X. L. Dong, H. Huang, Y. Y. Liu, W. N. Wang, X. G. Zhu, B. Lv, J. P. Lei and C. G. Lee, *Applied Physics Letters*, 2006, **89**, 053115.
7. N. C. Seeman, *Annual Review of Biochemistry*, 2010, **79**, 65-87.
8. A. El-Ansary and L. M. Faddah, *Nanotechnology, Science and Applications*, 2010, **3**, 65-76.
9. D. Deng, K. S. Novoselov, Q. Fu, N. Zheng, Z. Tian and X. Bao, *Nat Nano*, 2016, **11**, 218-230.
10. F. Yang, D. Deng, X. Pan, Q. Fu and X. Bao, *National Science Review*, 2015, **2**, 183-201.
11. M.-C. Daniel and D. Astruc, *Chemical Reviews*, 2004, **104**, 293-346.
12. I. Y. Wong, S. N. Bhatia and M. Toner, *Genes & Development*, 2013, **27**, 2397-2408.
13. J. R. Heath and M. E. Davis, *Annual Review of Medicine*, 2008, **59**, 251-265.
14. D. Janas and K. K. Koziol, *Carbon*, 2013, **59**, 457-463.
15. T. Dvir, B. P. Timko, D. S. Kohane and R. Langer, *Nat Nano*, 2011, **6**, 13-22.
16. S. Banta, Z. Megeed, M. Casali, K. Rege and M. L. Yarmush, *Journal of Nanoscience and Nanotechnology*, 2007, **7**, 387-401.
17. L. Lu, Y. Shen, X. Chen, L. Qian and K. Lu, *Science*, 2004, **304**, 422.
18. S. Hong and S. Myung, *Nat Nano*, 2007, **2**, 207-208.
19. D. D. L. Chung, in *Composite Materials: Functional Materials for Modern Technologies*, ed. D. D. L. Chung, Springer London, London, 2003, DOI: 10.1007/978-1-4471-3732-0\_3, pp. 55-71.
20. N. S. Dyadenko, A. I. Lun'ko and T. V. Kholoptseva, *Soviet Powder Metallurgy and Metal Ceramics*, 1973, **12**, 994-996.
21. J. M. Casstevens, H. G. Rylander and Z. Eliezer, *Wear*, 1978, **49**, 169-178.
22. C. Arnaud, F. Lecouturier, D. Mesguich, N. Ferreira, G. Chevallier, C. Estournès, A. Weibel and C. Laurent, *Carbon*, 2016, **96**, 212-215.
23. C. Guiderdoni, E. Pavlenko, V. Turq, A. Weibel, P. Puech, C. Estournès, A. Peigney, W. Bacsa and C. Laurent, *Carbon*, 2013, **58**, 185-197.
24. K. Rajkumar and S. Aravindan, *Wear*, 2011, **270**, 613-621.
25. K. Chu, H. Guo, C. Jia, F. Yin, X. Zhang, X. Liang and H. Chen, *Nanoscale Research Letters*, 2010, **5**, 868-874.
26. S. Cho, K. Kikuchi, T. Miyazaki, K. Takagi, A. Kawasaki and T. Tsukada, *Scripta Materialia*, 2010, **63**, 375-378.
27. S. J. Yoo, S. H. Han and W. J. Kim, *Carbon*, 2013, **61**, 487-500.
28. X. Gao, H. Yue, E. Guo, H. Zhang, X. Lin, L. Yao and B. Wang, *Powder Technology*, 2016, **301**, 601-607.
29. J.-f. Li, L. Zhang, J.-k. Xiao and K.-c. Zhou, *Transactions of Nonferrous Metals Society of China*, 2015, **25**, 3354-3362.
30. J. Dutkiewicz, P. Ozga, W. Maziarz, J. Pstruś, B. Kania, P. Bobrowski and J. Stolarska, *Materials Science and Engineering: A*, 2015, **628**, 124-134.
31. R. Jiang, X. Zhou, Q. Fang and Z. Liu, *Materials Science and Engineering: A*, 2016, **654**, 124-130.
32. H. Yue, L. Yao, X. Gao, S. Zhang, E. Guo, H. Zhang, X. Lin and B. Wang, *Journal of Alloys and Compounds*, 2017, **691**, 755-762.
33. W. Li, D. Li, Q. Fu and C. Pan, *RSC Advances*, 2015, **5**, 80428-80433.
34. Y. Chen, X. Zhang, E. Liu, C. He, C. Shi, J. Li, P. Nash and N. Zhao, *Scientific Reports*, 2016, **6**, 19363.
35. J. Shuai, L. Xiong, L. Zhu and W. Li, *Composites Part A: Applied Science and Manufacturing*, 2016, **88**, 148-155.
36. G. Xu, J. Zhao, S. Li, X. Zhang, Z. Yong and Q. Li, *Nanoscale*, 2011, **3**, 4215-4219.

37. C. Subramaniam, Y. Yasuda, S. Takeya, S. Ata, A. Nishizawa, D. Futaba, T. Yamada and K. Hata, *Nanoscale*, 2014, **6**, 2669-2674.
38. Y. Feng, G. E. McGuire, O. A. Shenderova, H. Ke and S. L. Burkett, *Thin Solid Films*, 2016, **615**, 116-121.
39. Y. L. Yang, Y. D. Wang, Y. Ren, C. S. He, J. N. Deng, J. Nan, J. G. Chen and L. Zuo, *Materials Letters*, 2008, **62**, 47-50.
40. C. Subramaniam, T. Yamada, K. Kobashi, A. Sekiguchi, D. N. Futaba, M. Yumura and K. Hata, *Nature Communications*, 2013, **4**, 2202.
41. C. Subramaniam, A. Sekiguchi, T. Yamada, D. N. Futaba and K. Hata, *Nanoscale*, 2016, **8**, 3888-3894.
42. G. Xie, M. Forslund and J. Pan, *ACS Applied Materials & Interfaces*, 2014, **6**, 7444-7455.
43. K. Jagannadham, *Metallurgical and Materials Transactions B*, 2012, **43**, 316-324.
44. K. Jagannadham, *Journal of Vacuum Science & Technology B, Nanotechnology and Microelectronics: Materials, Processing, Measurement, and Phenomena*, 2012, **30**, 03D109.
45. K. Jagannadham, *Metallurgical and Materials Transactions A*, 2013, **44**, 552-559.
46. C. Zhao and J. Wang, *physica status solidi (a)*, 2014, **211**, 2878-2885.
47. D. Zhang and Z. Zhan, *Journal of Alloys and Compounds*, 2016, **658**, 663-671.
48. S.-G. Cho and K.-C. Ko, *Thin Solid Films*, 2010, **518**, 6619-6623.
49. H. Udin, *J. Metals*, 1951, **3**.
50. P.-M. Hannula, J. Aromaa, B. P. Wilson, D. Janas, K. Koziol, O. Forsén and M. Lundström, *Electrochimica Acta*, **232**, 495-504.
51. P. Avouris, *Chemical Physics*, 2002, **281**, 429-445.
52. O. Hjortstam, P. Isberg, S. Söderholm and H. Dai, *Applied Physics A*, 2004, **78**, 1175-1179.
53. T. Dürkop, S. A. Getty, E. Cobas and M. S. Fuhrer, *Nano Letters*, 2004, **4**, 35-39.
54. Y. Feng and S. L. Burkett, *Computational Materials Science*, 2015, **97**, 1-5.
55. A. Dorri Moghadam, E. Omrani, P. L. Menezes and P. K. Rohatgi, *Composites Part B: Engineering*, 2015, **77**, 402-420.
56. A. Dorri Moghadam, B. F. Schultz, J. B. Ferguson, E. Omrani, P. K. Rohatgi and N. Gupta, *JOM*, 2014, **66**, 872-881.
57. E. Omrani, A. Dorri Moghadam, P. L. Menezes and P. K. Rohatgi, in *Ecotribology: Research Developments*, ed. J. P. Davim, Springer International Publishing, Cham, 2016, DOI: 10.1007/978-3-319-24007-7\_3, pp. 63-103.
58. M. Tabandeh-Khorshid, E. Omrani, P. L. Menezes and P. K. Rohatgi, *Engineering Science and Technology, an International Journal*, 2016, **19**, 463-469.
59. R. K. Khisamov, K. S. Nazarov, L. R. Zubairov, A. A. Nazarov, R. R. Mulyukov, I. M. Safarov, S. N. Sergeev, I. I. Musabirov, D. D. Phuong, P. V. Trinh, N. V. Luan, P. N. Minh and N. Q. Huan, *Physics of the Solid State*, 2015, **57**, 1206-1212.
60. A. K. Shukla, N. Nayan, S. V. S. N. Murty, K. Mondal, S. C. Sharma, K. M. George and S. R. Bakshi, *Materials Characterization*, 2013, **84**, 58-66.
61. A. K. Shukla, N. Nayan, S. V. S. N. Murty, S. C. Sharma, P. Chandran, S. R. Bakshi and K. M. George, *Materials Science and Engineering: A*, 2013, **560**, 365-371.
62. S. M. Uddin, T. Mahmud, C. Wolf, C. Glanz, I. Kolaric, C. Volkmer, H. Höller, U. Wienecke, S. Roth and H.-J. Fecht, *Composites Science and Technology*, 2010, **70**, 2253-2257.
63. D. Janas and K. Koziol, *Nanoscale*, 2016, **8**, 19475-19490.
64. K. Koziol, J. Vilatela, A. Moisala, M. Motta, P. Cunniff, M. Sennett and A. Windle, *Science*, 2007, **318**, 1892-1895.
65. J. J. Vilatela, R. Khare and A. H. Windle, *Carbon*, 2012, **50**, 1227-1234.
66. F. C. Nix and D. MacNair, *Physical Review*, 1941, **60**, 597-605.
67. Y. Sui, V. J. Gokhale, O. A. Shenderova, G. E. McGuire and M. Rais-Zadeh, *MRS Proceedings*, 2012, **1452**.
68. P.-M. Hannula, A. Peltonen, J. Aromaa, D. Janas, M. Lundström, B. P. Wilson, K. Koziol and O. Forsén, *Carbon*, 2016, **107**, 281-287.
69. S. Arai, T. Osaki, M. Hirota and M. Uejima, *Materials Today Communications*, 2016, **7**, 101-107.

70. S. Arai and T. Osaki, *Journal of The Electrochemical Society*, 2015, **162**, D68-D73.
71. M. Burda, A. Lekawa-Raus, A. Gruszczyk and K. K. Koziol, *ACS Nano*, 2015, **9**, 8099-8107.
72. L. Wang, Y. Cui, B. Li, S. Yang, R. Li, Z. Liu, R. Vajtai and W. Fei, *RSC Advances*, 2015, **5**, 51193-51200.
73. *Journal of Applied Physics*, 2011, **110**, 074901.
74. D.-B. Xiong, M. Cao, Q. Guo, Z. Tan, G. Fan, Z. Li and D. Zhang, *ACS Nano*, 2015, **9**, 6934-6943.
75. M. Park, B.-H. Kim, S. Kim, D.-S. Han, G. Kim and K.-R. Lee, *Carbon*, 2011, **49**, 811-818.
76. G.-x. Wu, Q.-y. Meng and C.-y. Wang, *Physica E: Low-dimensional Systems and Nanostructures*, 2011, **44**, 146-151.
77. M. Ghorbani-Asl, P. D. Bristowe and K. Koziol, *Physical Chemistry Chemical Physics*, 2015, **17**, 18273-18277.
78. G. Xuan, Z. Jie, W. S. Zhao and W. Gaofeng, 2016.
79. P. Sadowski, K. Kowalczyk-Gajewska and S. Stupkiewicz, *Composites Part B: Engineering*, 2015, **80**, 278-290.
80. F. Gao, J. Qu and M. Yao, *Applied Physics Letters*, 2010, **96**, 102108.
81. M. Rao, 2016.
82. A. Lekawa-Raus, T. Gizewski, J. Patmore, L. Kurzepa and K. K. Koziol, *Scripta Materialia*, 2017, **131**, 112-118.
83. A. Lekawa-Raus, J. Patmore, L. Kurzepa, J. Bulmer and K. Koziol, *Advanced Functional Materials*, 2014, **24**, 3661-3682.
84. D. Janas, A. C. Vilatela and K. K. K. Koziol, *Carbon*, 2013, **62**, 438-446.
85. D. Janas, A. Cabrero-Vilatela, J. Bulmer, L. Kurzepa and K. K. Koziol, *Carbon*, 2013, **64**, 305-314.
86. N. Khandoker, S. C. Hawkins, R. Ibrahim, C. P. Huynh and F. Deng, *Procedia Engineering*, 2011, **10**, 2572-2578.